



**AD-A274 895**



**THE DEVELOPMENT OF Cr,Tm,Ho:YAG LASERS FOR AIRBORNE LIDAR**

**John H. Flint**

**Schwartz Electro-Optics  
Research Division  
45 Winthrop Street  
Concord, MA 01742**

**22 February 1993**

**Final Report  
22 July 1991-21 January 1993**

**DTIC  
ELECTE  
JAN 12 1994  
S E D**

**Approved for public release; distribution unlimited**



**PHILLIPS LABORATORY  
Directorate of Geophysics  
AIR FORCE MATERIEL COMMAND  
HANSCOM AIR FORCE BASE, MA 01731-3010**

*29px*  
**94-01118**

**94 1 10 109**

"This technical report has been reviewed and is approved for publication"



STEVEN B. ALEJANDRO  
Contract Manager



DONALD E. BEDO, Chief  
Electro-Optical Environment Br



ROGER A. VAN TASSEL, Director  
Optical Environment Division

This report has been reviewed by the ESC Public Affairs Office (PA) and is releasable to the National Technical Information Service (NTIS).

Qualified requestors may obtain additional copies from the Defense Technical Information Center. All others should apply to the National Technical Information Service.

If your address has changed, or if you wish to be removed from the mailing list, or if the addressee is no longer employed by your organization, please notify PL/TSI; Hanscom AFB MA 01731-3010. This will assist us in maintaining a current mailing list.

Do not return copies of this report unless contractual obligations or notices on a specific document requires that it be returned.

# REPORT DOCUMENTATION PAGE

*Form Approved*  
OMB No. 0704-0188

Public reporting burden for this collection of information is estimated to average 1 hour per response, including the time for reviewing instructions, searching existing data sources, gathering and maintaining the data needed, and completing and reviewing the collection of information. Send comments regarding this burden estimate or any other aspect of this collection of information, including suggestions for reducing this burden, to Washington Headquarters Services, Directorate for Information Operations and Reports, 1215 Jefferson Davis Highway, Suite 1204, Arlington, VA 22202-4302, and to the Office of Management and Budget, Paperwork Reduction Project (0704-0188), Washington, DC 20503

<b>1. AGENCY USE ONLY (Leave blank)</b>	<b>2. REPORT DATE</b> 22 February 1993	<b>3. REPORT TYPE AND DATES COVERED</b> Final Report(22 Jul 1991-21 Jan 1993)
---	---	--

<b>4. TITLE AND SUBTITLE</b> The Development of Cr, Tm, Ho: YAG Lasers for Airborne Lidar	<b>5. FUNDING NUMBERS</b> PE 35160F PR 7670 TA 16 WU BB Contract F19628-91-C-0119
--	--

<b>6. AUTHOR(S)</b> John H. Flint	
--------------------------------------	--

<b>7. PERFORMING ORGANIZATION NAME(S) AND ADDRESS(ES)</b> Schwartz Electro-Optics, Inc Research Division 45 Winthrop Street Concord, MA 01742	<b>8. PERFORMING ORGANIZATION REPORT NUMBER</b>
---	---

<b>9. SPONSORING/MONITORING AGENCY NAME(S) AND ADDRESS(ES)</b> Phillips Laboratory 29 Randolph Road Hanscom AFB, MA 01731-3010  Contract Manager: S. Alejandro/GPOA	<b>10. SPONSORING/MONITORING AGENCY REPORT NUMBER</b>  PL-TR-93-2035
--	--

**11. SUPPLEMENTARY NOTES**

<b>12a. DISTRIBUTION / AVAILABILITY STATEMENT</b> Approved for public release; distribution unlimited	<b>12b. DISTRIBUTION CODE</b>
--	-------------------------------

**13. ABSTRACT (Maximum 200 words)**  
We proposed a research effort to determine the physical principals limiting the performance of pulsed Cr,Tm,Ho:YAG (CTH:YAG) lasers. The project was to conclude with the design of an eye-safe, aircraft-based transmitter for LIDAR and other remote sensing applications. The target specifications of the laser were: 100 mJ at 10 Hz repetition rate, single longitudinal mode, with a minimum pulse width of 500 ns. The research program investigated Q-switched operation of CTH:YAG lasers, flashlamp-pumped amplifiers, and injection seeding using diode-laser-pumped, single-frequency TH:YAG lasers. We extracted up to 30 mJ in a TEM<sub>00</sub> pulse at 10 Hz from both linear and ring resonators. The pulse widths at 30mJ ranged from 200 ns to 400 ns. We demonstrated injection-seeding of a ring resonator operating at 10 mJ per pulse at 7 Hz, and amplified the output of this laser by a factor of three. The final task of this research program, the design of an aircraft-based transmitter, was incomplete at the end of the contract period.

<b>14. SUBJECT TERMS</b> Lasers                      Holmium                      Injection-seeding LIDAR                      Laser amplifiers	<b>15. NUMBER OF PAGES</b> 30
	<b>16. PRICE CODE</b>

<b>17. SECURITY CLASSIFICATION OF REPORT</b> Unclassified	<b>18. SECURITY CLASSIFICATION OF THIS PAGE</b> Unclassified	<b>19. SECURITY CLASSIFICATION OF ABSTRACT</b> Unclassified	<b>20. LIMITATION OF ABSTRACT</b> SAR
--	---	--	--

## Table of Contents

1	Introduction and Background .....	1
2	Technical Objectives .....	4
3	Research Conducted and Results .....	4
3.1	Task 1. Cr,Tm,Ho:YAG Oscillator .....	4
3.1.1	FTS Chiller and Fluorinert FC-104 .....	5
3.1.2	Close-Coupled Pump-Cavities .....	7
3.1.3	Elliptical Reflector Pump-Cavity .....	8
3.1.4	Linear Laser Resonator .....	8
3.1.5	Ring Laser Resonator .....	14
3.2	Task 2. Injection Seeding .....	15
3.2.1	Seed Laser .....	15
3.2.2	Injection-Seeded Ring-Laser .....	17
3.3	Task 3. Amplifier .....	22
3.4	Task 4. Lidar Transmitter Design .....	26
4	References .....	26

Accession For	
NTIS CRA&I	<input checked="" type="checkbox"/>
DTIC TAB	<input type="checkbox"/>
Unannounced	<input type="checkbox"/>
Justification .....	
By .....	
Distribution /	
Availability Codes	
Dist	Avail and/or Special
A-1	

DTIC QUALITY INSPECTED 5

# 1 Introduction and Background

There are several remote sensing applications of extreme interest to the U.S. Air Force. Space-based wind velocity measurement to provide data for global weather modeling and forecasting is perhaps the most ambitious. Others include aerosol ranging and optical path characterization from aircraft, as well as wind velocity and especially wind shear measurements, also from aircraft. Pulsed single-frequency lasers have been proposed for these applications, and several gas-laser systems have been flown on large aircraft test-beds. Solid-state lasers offer the promise of greater reliability, significantly smaller size and lighter weight, but the most highly developed solid-state lasers based on the  $Nd^{3+}$  ion are not considered to be eye-safe. The holmium laser is an alternative solid-state laser using the  $Ho^{3+}$  ion, which emits  $2.1 \mu m$  radiation. This laser is currently under development at Schwartz Electro-Optics, Inc. and elsewhere. Co-doping holmium with chromium and thulium in a YAG host allows flashlamp excitation with reasonable efficiency, but to date, even the performance of laboratory, table-top, holmium lasers lags behind what would be required of a miniaturized, ruggedized, flyable laser.

We proposed a research effort to determine the physical principles limiting the performance of pulsed Cr,Tm,Ho:YAG (CTH:YAG) lasers. The findings were to allow the design and construction of an eye-safe, aircraft-based transmitter for LIDAR and other remote sensing applications. The research results were also expected to indicate what steps would be required to make construction of a diode-laser pumped transmitter both feasible and economical.

The technical specifications of an aircraft-based, holmium-laser transmitter will of course depend on the specific application, but in general the requirements listed in Table 1 under the "DESIRED" column should be met:

Table 1. Technical specifications of Q-switched holmium lasers.

SPECIFICATION	DESIRED	STATE OF THE ART	
		SEO	CTI
Energy per pulse (mJ)	100	20	50
Pulse width ( $\mu sec$ )	0.5-1	0.6	0.15
Repetition rate (Hz)	10	4	3
Mode quality	$TEM_{00}$	$TEM_{00}$	$TEM_{00}$

Also listed in Table 1 are the best values current at the beginning of this project for Q-switched holmium lasers built by the SEO Research Division, and by Coherent Technologies, Inc. (CTI) [1]. In addition, the laser must be compact, efficient and rugged enough to maintain alignment through hard landings and in-flight turbulence.

Although it appears from Table 1 that the desired specifications are only marginally greater than the current state of the art, the peculiar properties of holmium-thulium co-doped lasers make closing the gap much more difficult than might otherwise be expected. Holmium lasers suffer from ground-state absorption, a low stimulated-emission cross section and an upconversion process that limits energy storage. The excited energy is shared not only by the 15 sub-levels of the  $^5I_7$  holmium multiplet, but also by the  $^3F_4$  multiplet of thulium, from which energy transfer is too slow to be useful for Q-switched pulses. Design trade-offs meant to lengthen the pulse tend to make the lasers unstable or force operation dangerously near the optical damage threshold.

Perhaps the largest problem with holmium lasers is that the lower level of the laser transition is part of the ground-state manifold, and therefore it has a small but significant population that has to be overcome before the laser will reach threshold. This is referred to as ground-state absorption, and is often described as a saturable loss that increases the laser threshold, but does not affect the laser slope efficiency. At room temperature, the absorption ranges from 0.3-1.1% /mm for the three strongest laser lines [2], due to the presence of about 1% of the holmium ions in the lower laser levels. Due to the splitting of the upper level only 10% of the excited Ho ions are in the upper laser level, so just to reach threshold 10% of the ions must be excited to balance the ground state population. This works out to be  $5 \times 10^{18} / \text{cm}^3$  for the standard dopant concentration, and is responsible for the 40-80 J thresholds encountered when flashlamp pumping CTH:YAG. Lowering the crystal temperature reduces the threshold by reducing the thermally excited population at the lower laser levels. The reduction in population is governed by the Boltzmann distribution, and changes slowly with temperature near 300 K. However, lowering the laser threshold only slightly improves the overall performance by also reducing the heat load on the laser crystal and by reducing the upper-state density required for a given amount of net gain, which limits the effects of up-conversion. Lower temperatures also shift the energy sharing between the holmium and thulium excited states in favor of the holmium states. Again, the change is slow with temperature, but the cumulative effect of lowering the crystal temperature from 22°C to -24°C in a cw, Ti:Al<sub>2</sub>O<sub>3</sub>-laser-pumped Tm,Ho:YAG laser was to reduce the threshold by a factor of three.

The second major problem with holmium is a rather low stimulated-emission cross-section ( $\sigma$ ). Effective cross-sections for the strongest lines range from  $4 \times 10^{-21} \text{ cm}^2$  to  $1.4 \times 10^{-20} \text{ cm}^2$  at room temperature. [2] Lowering the temperature increases the values slightly since the effective cross-section is the product of  $\sigma$  and the level occupation. To generate a small-signal gain coefficient,  $g_0$ , of only  $0.14 \text{ cm}^{-1}$  requires an inversion density of  $10^{19} \text{ cm}^{-3}$  which is 20% of the holmium in a standard composition rod. Over 10 cm, this produces a net gain of four.

The third problem is an up-conversion mechanism that reduces the apparent upper-state lifetime from 8-10 ms at low excitation levels to less than 1 ms at the inversion densities needed for Q-switched lasers and amplifiers. This results in the need to use pump-pulses that are 250-500  $\mu\text{s}$  long, which is not a concern for flashlamp-pumping, but which severely limits diode-laser-pumped applications. Lowering the temperature seems to have little effect on the upconversion rate itself, although lower temperatures reduce the upper-state density required for a given amount of gain by reducing the ground-state density thus reducing the total amount of up-conversion. Energy removed from the upper state by up-conversion is converted to heat which must be removed by the cooling system.

Finally, there are several issues in building Q-switched lasers that are at cross-purposes with reaching our target specifications. One involves the relationships among energy storage, gain and Q-switched pulse width. Pumping harder to store more energy before the Q-switch is opened in order to increase the energy per pulse results in the laser operating at larger values of gain which results in a shorter output pulse. We found that when extracting 20 mJ the pulse-width was already 600 ns, near the minimum desired width. Lowering the rod temperature will lower the lamp energy required to extract 20 mJ, but it will not change the relationship between gain and pulse-width. Operating the laser with a smaller degree of out-coupling will drive the circulating intra-cavity power even closer to the damage threshold, and further lengthening the laser cavity will increase diffraction losses making the cavity more sensitive to vibrations and more difficult to stabilize. A slowly opening Q-switch will produce a longer Q-switched pulse with less energy per pulse.

We concluded that it is unlikely that much more than 20 mJ of energy can be extracted from a Q-switched CTH:YAG oscillator with a pulse-width of 500 ns or more. Our approach to meeting the target specifications was therefore to build a 10-Hz, injection-seeded oscillator that produced 500-ns pulses with as much energy as possible, and then to amplify these pulses to 100 mJ with a flashlamp-pumped amplifier. Cooling the oscillator and amplifier to as low as

-40°C was to make 10-Hz operation possible by significantly reducing the thermal loading due to ground-state absorption. The design of a ruggedized, flyable, LIDAR transmitter was to begin once the laboratory version had been demonstrated.

## 2 Technical Objectives

The proposed research effort consisted of the following elements to be performed over eighteen months.

- 1) Develop a 10-Hz, TEM<sub>00</sub>, flashlamp-pumped CTH:YAG oscillator with at least 20 mJ output energy in a 0.5-1 μs pulse. The resonator must be short and stable, suitable for ruggedization.
- 2) Demonstrate single-longitudinal-mode, injection-seeding of the oscillator developed in Task #1.
- 3) Develop a flashlamp-pumped amplifier capable of increasing the output of the above oscillator to 100 mJ/pulse, while preserving its TEM<sub>00</sub>, SLM quality.
- 4) Design a ruggedized LIDAR transmitter incorporating a diode-pumped SLM seed-laser, a Q-switched oscillator, and an amplifier. Target specifications are 100 mJ at 10 Hz, SLM, TEM<sub>00</sub>, with a pulse-width between 500 ns and 1 μs. The transmitter was to be constructed under a follow-on contract.

## 3 Research Conducted and Results

The research efforts devoted to the tasks outlined in the previous section are described in detail below:

### 3.1 Task 1. Cr,Tm,Ho:YAG Oscillator

- 1) *Develop a 10-Hz, TEM<sub>00</sub>, flashlamp-pumped CTH:YAG oscillator with at least 20 mJ output energy in a 0.5-1 μs pulse. The resonator must be short and stable, suitable for ruggedization.*

The objective of the first task was to increase the repetition rate of our Q-switched CTH:YAG laser from 4 Hz to 10 Hz, without affecting the mode quality or pulse width. Our primary approach was to reduce the temperature of the laser rod from around 10°C to as low as

-40°C, thereby reducing the laser threshold and the flashlamp energy required to extract 20 mJ in a 500 ns pulse. We expected this cooling would reduce the threshold to 1/3 of the 10°C value, so that a total of 20-25 J of lamp energy would be required per pulse.

We built an hermetic enclosure to surround an SEO close-coupled, silver-reflector pump cavity. The cooling was provided by an FTS Systems recirculating cooler using Fluorinert, a low viscosity fluorocarbon. Several close-coupled cavities were tested in a linear, acousto-optically Q-switched laser resonator, as well as in a ring-resonator. In addition, we tested an elliptical reflector pump-cavity we purchased from Kentek, Inc., which could only be cooled with water. Several of the close-coupled cavities produced up to 30 mJ of energy in a single TEM<sub>00</sub> pulse at 10 Hz, although the pulse-width was considerably shorter than our target. The performance of the ring-resonator was not as promising.

### **3.1.1 FTS Chiller and Fluorinert FC-104**

The primary innovation of this effort that was designed to allow 10-Hz operation of a CTH:YAG laser was to cool the laser rod significantly below 0°C, but without going to the complexity of using liquid nitrogen. Previous work had suggested that cooling only to -40°C would significantly reduce the laser threshold. We determined that a reasonably straight-forward approach would be to use a commercially available recirculating cooler charged with Fluorinert, a low viscosity fluorocarbon, coupled to standard SEO-developed close-coupled pump-cavities. Fluorinert has a viscosity at -40°C that is similar to that of liquid water, and has a net heat-transfer coefficient that is only a factor of two or so smaller. We therefore expected to find 30-50 psi pressure drops in the Fluorinert-cooled system. In addition, Fluorinert is chemically benign, non-toxic and nonflammable, and available in a highly purified version, FC-104, which is unaffected by UV radiation. In comparison, ethylene glycol/water mixtures have extremely large viscosities at low temperatures, and tend to decompose under UV irradiation, producing an acidic liquid that can be quite aggressive.

We purchased the recirculating cooler, Model RC-100C-L02, from FTS, Inc., after considerable discussion. The chiller was designed for an ultimate low temperature of -40°C, with a specified heat-removal of 900 W at -20°C, and was tested at the factory charged with Fluorinert. It included a 4-GPM positive-displacement pump, a water-cooled condenser, a high-pressure by-pass, and a pressure gauge as options. Materials in contact with the Fluorinert include neoprene hose, and copper, brass and stainless steel.

The chiller was coupled to the pump-cavities with additional plumbing provided by SEO. From the literature provided by 3M, there was some question as to the compatibility of Fluorinert with brass and copper due to its ability to dissolve water and oxygen. We therefore constructed the particle-filter manifold and entrance-temperature monitor from stainless-steel components whereas the exit-temperature monitor and the flow-switch were of brass. We initially used reinforced neoprene hose for the interconnections, but we found that it became extremely stiff at low temperatures, which coupled pump-vibrations to the optical table. We subsequently found that reinforced silicone hose retained its flexibility at  $-40^{\circ}\text{C}$ . Our compatibility concerns proved to be unfounded as we never detected any signs of corrosion on any of the components that were in contact with Fluorinert. In fact the silver reflectors from the close-coupled cavities looked as if they had been recently polished even after several months of operation.

Two significant problems were encountered while working with the Fluorinert cooling system. The first was that the recirculating cooler was extremely noisy, especially when operated at low temperatures. The second was that it was difficult to make leak-free coolant connections, and leaks were hard to pinpoint. Together, these two rather mundane problems cost us a significant amount of time. We traced the noise to the positive-displacement pump in the chiller, and attempted to get FTS to quiet it down. After several service visits under the chiller warranty they finally told us that the noise was normal, and suggested we move the chiller to a remote location. As this would have increased the pressure-drop and heat-gain in the recirculating lines, we decided instead to enclose the chiller in an anechoic box, which seemed practical since the condenser was water-cooled. This reduced the noise considerably, but it also caused the air-cooled compressor to overheat. We ended up mounting two small fans over holes cut in the back of the box to blow room-air over the compressor, and found that with the box-cover partially removed the noise was bearable, and the chiller would not over-heat. A possible alternative that will be explored if we ever contemplate purchasing a similar chiller is to replace the pump with a smaller, better insulated model.

The problem of locating and sealing leaks was partially anticipated from the 3M literature, as we purchased a halogen leak detector designed for the refrigeration industry. This proved quite capable of indicating the presence of a leak, but not of identifying its precise location. As the Fluorinert would evaporate instead of forming droplets, we finally had to resort to pressurizing the system with dry nitrogen and looking for bubbles with SNOOP™. In retrospect we should have included isolation valves on the chiller input and output ports to allow pressurization of new pump-cavities. The most troubling source of leaks were the barbed fittings on the pump-cavity bases, where we could not tell if the leaks were past the barbs or past the

pipe-fittings in the base. As these leaks were inside the hermetic enclosure, and seemed to get worse as the temperature was reduced, we spent a lot of time trying to eliminate them. A possible solution for the future is to use hose with permanently bonded fittings. One supplier of silicone hose is working on such a design but does not now have a product.

### 3.1.2 Close-Coupled Pump-Cavities

Several close-coupled, silver-reflector, pump cavities were purchased from the SEO Solid State Laser Division in Orlando, Florida. The pump-cavity design evolved over time as it was optimized for a high-average power, normal-mode, medical application. This caused us some confusion as we did not discover that changes had been made to the design until after we had received the latest version. It turned out that for our application the first delivered pump-cavity configuration was the best.

**Table 2.** Close-coupled pump-cavities.

Property	Version 1	Version 2	Version 3	Version 4
Coolant Flow	Sequential	Parallel	Parallel	Parallel
Coolant Connections	3/8"	1/2"	1/2"	1/2"
Pressure Drop	50 psi@2 Gpm	30 psi@4 Gpm	30 psi@4 Gpm	30 psi@4 Gpm
Threshold	Highest	Low	Lowest	Intermediate
Mode Quality	Good	Poor	Poorest	Good

The close-coupled cavities consist of a titanium reflector-housing kinematically mounted to a *Delrin* insulator-base. A total of four different pump-cavity configurations were tested at various times, assembled from two different bases and three different reflector geometries. Table 2 presents the differences among the four configurations. All of the cavities were loaded with 4x100 mm Cr,Tm,Ho:YAG laser rods and 4 mm-I.D. Xenon flashlamps. In the first cavity we tested, Version 1, the coolant was first directed along the laser rod, then back through the pump-cavity along the flashlamp, before returning to the chiller. A Pyrex plate separated the two flows. As this results in a relatively large pressure-drop across the pump-cavity, we limited the coolant flow to approximately 2 Gpm. Nevertheless the Pyrex plate would soon fracture and bow out until it came into contact with the flashlamp. We therefore switched to the parallel-flow configuration, Versions 2 and 3, where the coolant is split into two streams in the base. One is directed along the rod, the other along the lamp. This configuration was operated at the

maximum coolant flow of 4 Gpm. When it became clear that Version 1 produced superior laser performance, we combined the advantages of both versions by placing the Version 1 reflectors on the parallel-flow base, to form Version 4.

### 3.1.3 Elliptical Reflector Pump-Cavity

By the time we had tested pump-cavity Versions 1-3 we became somewhat discouraged with our lack of progress. The laser thresholds had decreased, but at the same time the laser performance deteriorated, presumably because of pump nonuniformity. We decided to try a completely different cavity design and purchased an elliptical reflector pump-cavity from Kentek, Inc. This cavity employs flow-tubes around the laser rod and the flashlamp, and back-cools the silver-coated glass reflectors. As the air-space inside the cavity is not readily purgeable and the cavity was not designed to be compatible with Fluorinert, we decided to operate it with water cooling. When the laser performance with the Kentek cavity turned out to be no better than with Version 2, we went back to the close-coupled cavities for the final experiments. One potential advantage of flow-tube cavities that we did not have time to exploit is that different coolants at different temperatures could be used.

### 3.1.4 Linear Laser Resonator

The bulk of the oscillator development employed the nearly symmetric linear laser resonator illustrated in Figure 1. The output coupler was 39 cm from one end of the laser rod, and the rear reflector was located 45 cm from the other rod end. Aerotech AOM110-2 high resolution, gimbal mounts were used for the resonator mirrors. An IntraAction Corp. acousto-optic Q-switch was placed between the laser rod and the rear reflector. Also shown in Figure 1 are the AR-coated windows sealing the pump-cavity hermetic enclosure. The mirror mounts, the Q-switch bracket, and the hermetic enclosure were bolted directly to a 2'x4' Invar breadboard for thermal and mechanical stability.

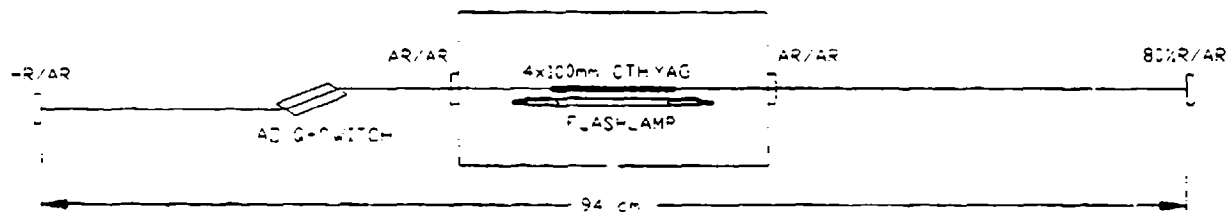
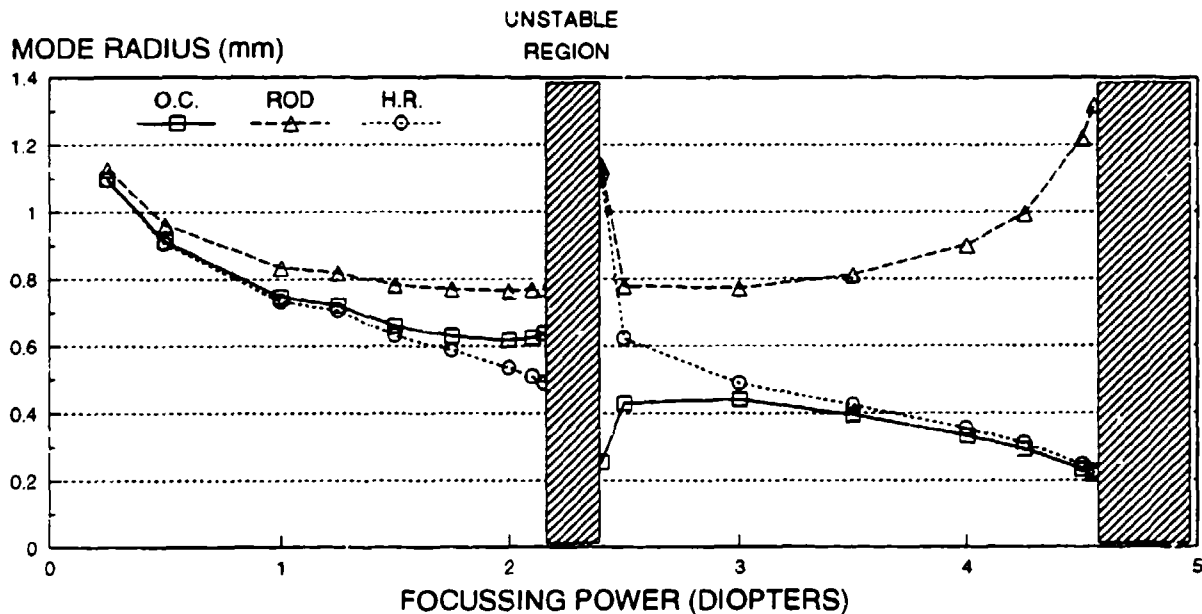


Figure 1. Schematic diagram of the linear resonator.

We used a computer program called CAV8 to calculate the laser mode size at various points in the linear cavity as a function of the thermally induced lens in the laser rod. Figure 2 shows how the laser mode at the center of the rod and at the two mirrors varies as the thermal lens increases to 4.5 diopters. Note the two broad regions where the mode-size in the rod is nearly constant, and how the mode at the mirrors becomes quite small as the regions of instability are approached. This latter feature is a particular problem for Q-switched lasers as the small mode-size produces high power-densities, leading to damage.



**Figure 2.** Calculated laser mode-size as a function of rod diopter at the center of the rod and at the resonator mirrors for the linear cavity.

Figure 3 presents the laser performance of the linear resonator as originally assembled with the Version 1 pump-cavity. The laser was operated at 10 Hz with a 500  $\mu$ s current pulse, and the Q-switched laser mode was TEM<sub>00</sub>. The 5°C data-set was collected with water-cooling and no AR-coated windows in the resonator as the Fluorinert system was still under construction. We were able to extract nearly 30 mJ with a 400-ns pulse width. Cooling to -35°C reduced the threshold by a factor of two, and shortened the 30-mJ pulse-width to 300 ns. At only slightly higher pump-levels the laser performance became erratic, presumably because the thermal lens was in the unstable range just over 2 diopters as shown in Figure 2. When the laser stabilized, we had to shorten the length of time the Q-switch was open to suppress a second pulse, and the resulting pulse-width was less than 200 ns.

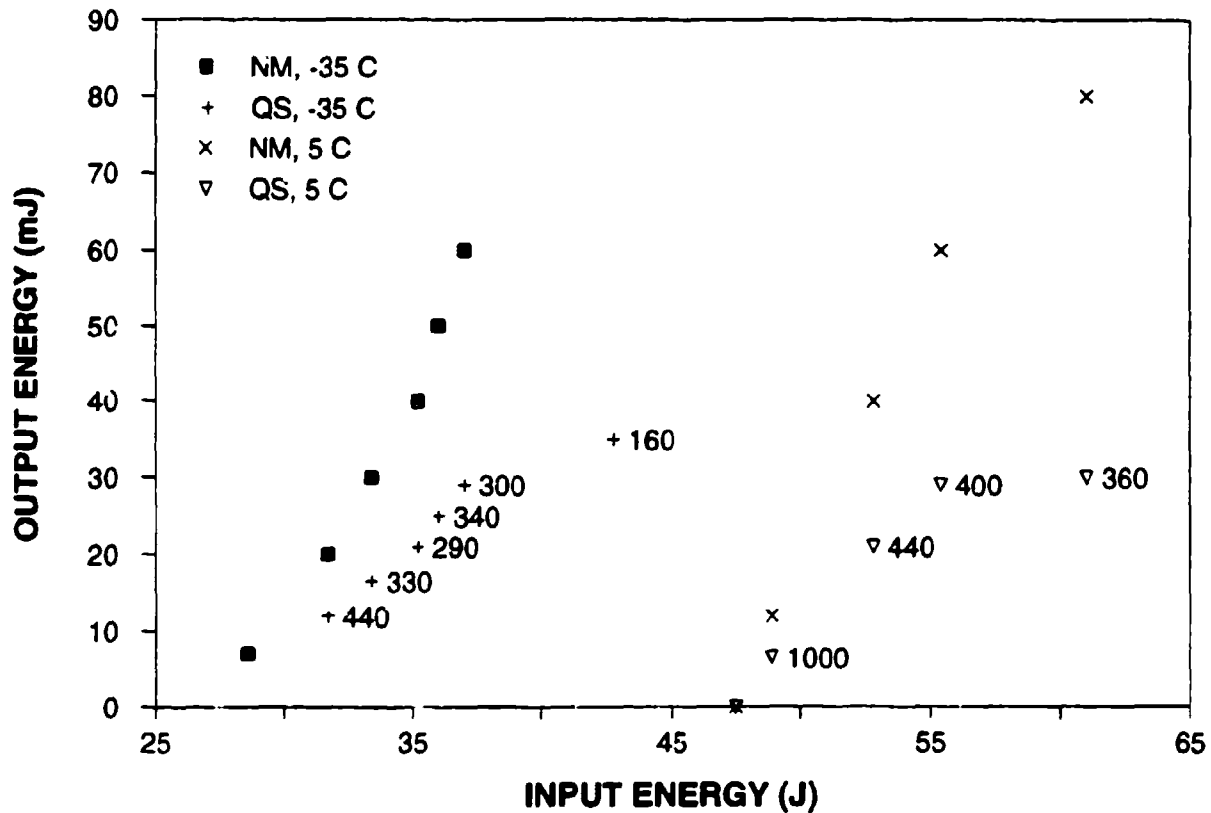


**Figure 3.** Normal mode and Q-switched performance at 10 Hz of the linear resonator using the Version 1 pump-cavity. The numbers next to the data points are the FWHM duration of the Q-switched pulse in ns.

Figure 4 presents the laser performance of the linear resonator configured with the Version 2 pump-cavity. Both data sets were collected using Fluorinert cooling and with the AR-coated windows in the laser cavity. Figure 4 shows that although the laser threshold was significantly lower than when using Version 1, the laser only produced 15 mJ at 5°C, and less than 20 mJ with a reasonable pulse-width at -35°C. The unstable region, which had been around 38-42 J, now appeared around 27-30 J. When we tested the Version 3 pump-cavity, we found that its normal-mode performance was so poor that we never bothered to Q-switch it.

The performance of two different laser rods is compared in Figure 5. The data was collected using the Version 1 pump cavity, cooled with *Fluorinert* to -35°C. Figure 5 shows that using the reduced thulium concentration rod, H1102, instead of rod H855, increased the laser threshold, while the ratio of Q-switched energy to normal-mode energy at a given input energy was unchanged. We concluded that the increased threshold may have been due to a lower than

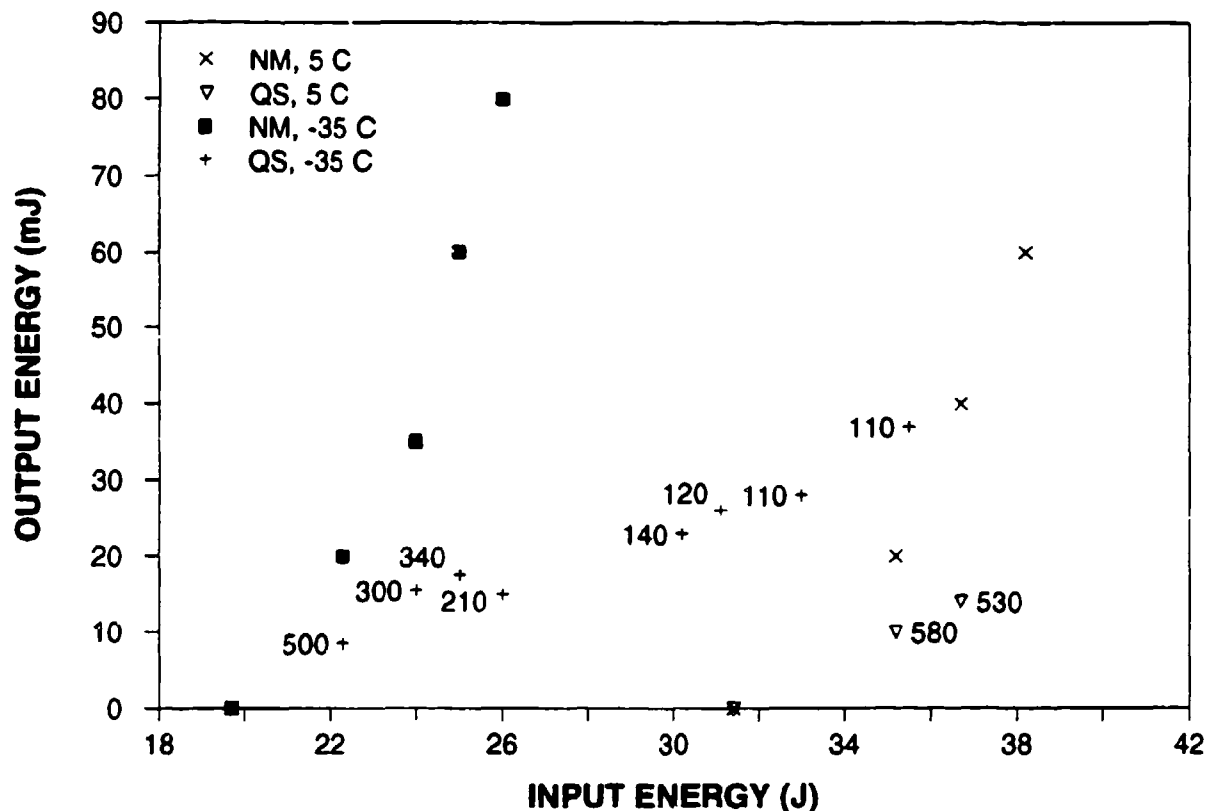


**Figure 4.** Normal mode and Q-switched performance at 10 Hz of the linear resonator using the Version 2 pump-cavity. The numbers on the figure are the FWHM in ns of the Q-switched pulse.

expected chromium concentration, and had a second low thulium rod fabricated, this time from the high chromium end of the boule. This rod was tested in pump-cavity Version 2 at 5°C. Again, the laser threshold was higher, although now up to 20 mJ could be extracted before the laser became unstable, which was an improvement over the H855 performance in Version 2. However, the pulse was short, and the energy was low compared to the 30 mJ extracted from H855 in cavity Version 1.

All of the laser performance data reported above was collected using the laser resonator shown in Figure 1 consisting of two flat mirrors spaced 94-cm apart, with the laser rod approximately in the center. The laser mode radius in the rod depends on the magnitude of the thermal lens induced in the rod, and has two broad minima at 0.8 mm according to Figure 2. We reasoned that if we could increase the mode radius to 1.3 mm (1/3 of the rod diameter), then the pulse energy would increase by a factor of three, with no change in pulse width. Our first

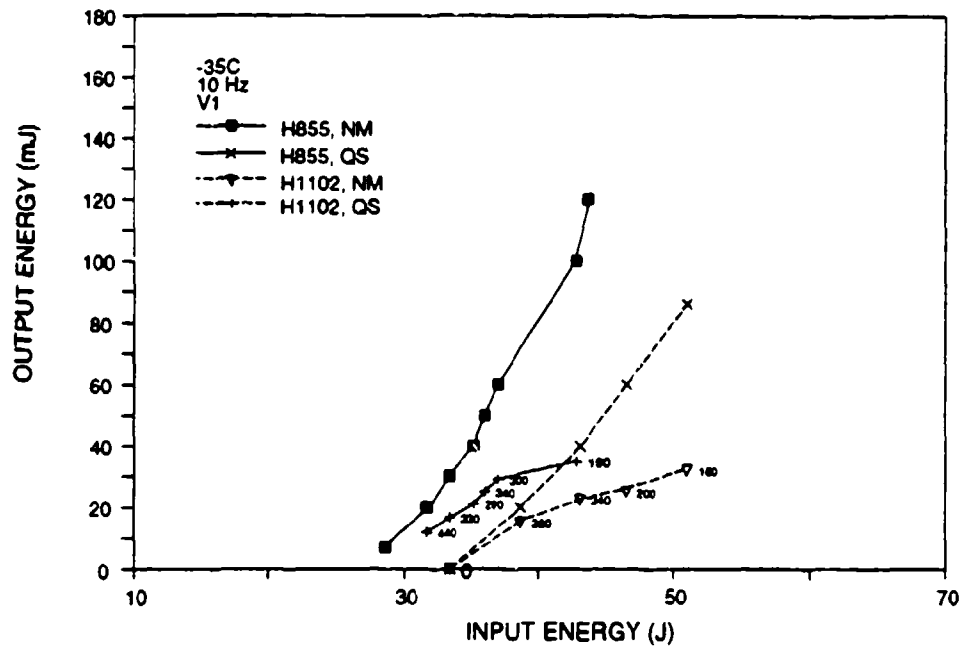


Figure 5. Laser performance at 10 Hz and -35°C of the "standard" Cr,Tm,Ho:YAG laser rod, H855, and the first low thulium rod, H1102, in pump cavity Version 1.

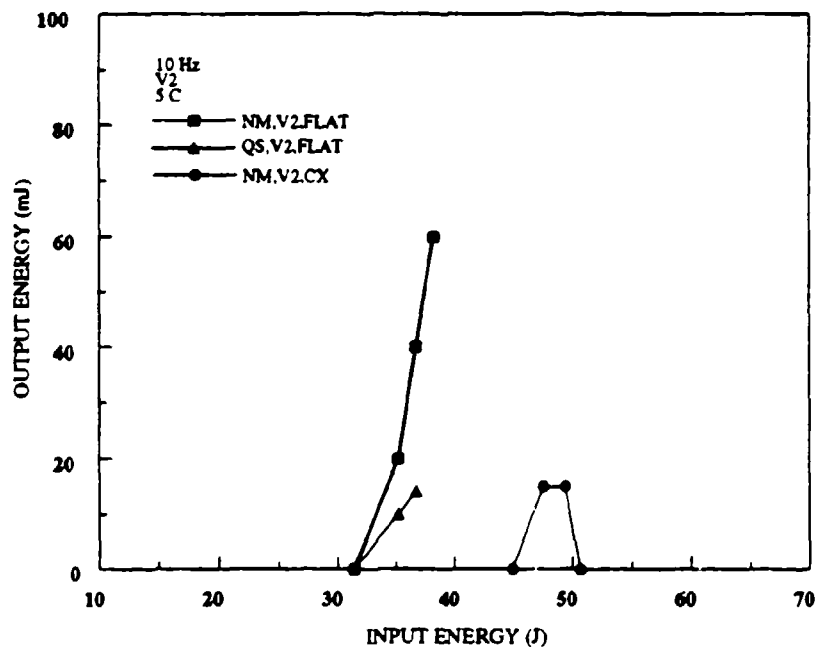
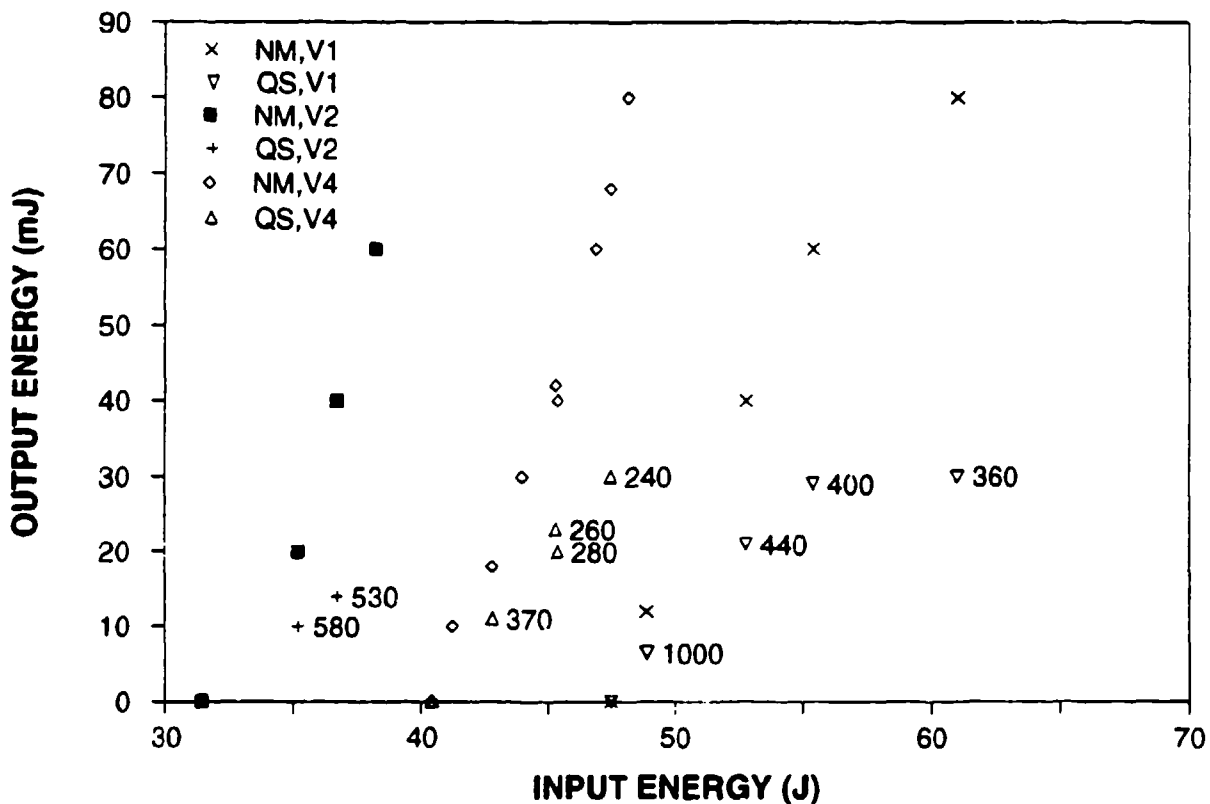


Figure 6. Laser performance at 10 Hz and 5°C of the "standard" Cr,Tm,Ho:YAG laser rod, H855, in flat/flat and convex/convex cavities.

attempt to increase the mode size was not very promising, as shown in Figure 6. The laser cavity employed two 1-m radius-of-curvature convex mirrors in place of the flats, and the mode radius was calculated to be about 1 mm. The laser performance was very disappointing, both in terms of laser power and sensitivity to misalignment. We did not pursue this approach since it is hard to see how the curved mirror cavity could be converted to a ring resonator.



**Figure 7.** Normal mode and Q-switched performance at 10 Hz and 5°C of the linear resonator using pump-cavities Versions 1, 2, and 4. The numbers on the figure are the FWHM in ns of the Q-switched pulse.

We were finally forced to conclude that neither low thulium-concentration laser rods nor more exotic laser resonators or pump-cavities would produce improved laser performance over what we had demonstrated with pump-cavity Version 1. Since operating at 5°C kept the pulse-width closer to our 500 ns target, we decided to use water cooling for the oscillator, and built a new laser resonator around pump-cavity Version 4. We took advantage of the low winter humidity and avoided the hermetic enclosure with its lossy windows. Figure 7 compares the performance of this laser to the 5°C data collected using pump-cavities Version 1 and Version 2.

The Version 4-laser threshold was 40 J, and we were able to extract 30 mJ at 10 Hz. The laser pulse-width was shorter than when cavity Version 1 was used, but we decided that it was long enough. We are developing an actively controlled Q-switch under a different research program which can be applied to this laser in the future if longer pulses are absolutely required.

### 3.1.5 Ring Laser Resonator

The ring resonator, shown in Figure 8, was also constructed directly on the Invar breadboard. The output coupler and the PZT-mounted HR were hard-mounted, that is held in rigid, non-adjustable mounts. The other two HR mirrors were mounted in Aerotech AOM110-2 gimbal mounts. This arrangement provided the four degrees of freedom required to align the ring resonator, while allowing the bulky PZT to be held stiffly. The thin-film polarizer was only added in the final phase of the injection-seeding experiments, described below. The ring-resonator was aligned using first a diode-laser pumped Nd:YAG laser, then later a 850-nm diode laser. As expected, the ring was significantly more alignment-sensitive than the linear resonator, with walking both mirrors being usually required. Precise adjustment of the AO Q-switch Bragg angle also required cavity optimization. The total cavity length ended up being 1 m, slightly longer than the linear resonator. This results in a cavity mode-spacing around 300 MHz, which proved to be almost outside the bandwidth of the InGaAs detector.

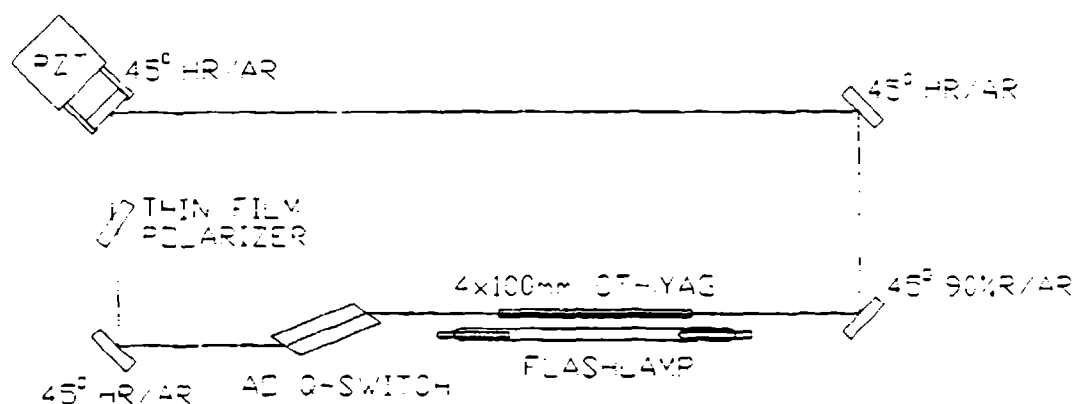


**Figure 8.** Schematic drawing of the ring resonator.

The laser performance of the ring proved to be rather disappointing when compared to the performance of the linear resonator. The laser threshold was significantly higher, the Q-switched pulse-width shorter, and the mode-quality would break-up at what seemed like a relatively low average power. It turned out that part of the problem was that the so-called HR mirrors were in fact only 99% R for the "p" polarization, which was the laser polarization determined by the AO

Q-switch. Rotating the Q-switch to make the laser "s" polarized on the mirrors would have made the ring nonplanar due to the beam-jog in the Brewster angle piece. The 1% loss per mirror adds up to 3% per pass since the ring has three nominally HR surfaces. This is 30% of the output coupler transmission of 10%. We were able to extract a total of 30 mJ at 10 Hz from the ring using the Version 4 pump-cavity cooled with water to 5-10°C, but only 24 mJ was through the output coupler, 10 mJ in one direction, 14 mJ in the other. The pulse-width was 200 ns, and the mode quality was nominally TEM<sub>00</sub>, although it required a good deal of cavity adjustment to keep the mode from turning into two lobes, one above the other. This performance was judged sufficient to begin the injection-seeding experiments.

### **3.2 Task 2. Injection Seeding**

*2) Demonstrate single-longitudinal-mode, injection-seeding of the oscillator developed in Task #1.*

The objective of the second task was to demonstrate SLM injection-seeding of the resonator developed in Task #1. We had intended to use a tunable single-frequency, diode-pumped, Tm,Ho:YAG ring-laser developed during the AFGL Phase II SBIR for the seed laser, so CW development was not supposed to be part of this effort. Unfortunately, we determined that the frequency-stability of this laser was not sufficient for it to be used as a seed-source. As a ruggedized CW laser was under development under different sponsorship, we decided to modify a standing-wave laser to incorporate some of the new features. We successfully injection-seeded the ring-resonator developed under Task #1 using this laser, and in the process determined that a different seed-laser design should be evaluated before a complete system is designed.

#### **3.2.1 Seed Laser**

The seed laser constructed for this task is illustrated in Figure 9. The hemispherical resonator is formed by the flat HR/HT mirror and a 10-cm radius-of-curvature output coupler (0.5%T). Both mirrors are hard-mounted to the resonator for improved frequency stability. The laser crystal, a 5-mm-diameter, 3-mm-thick piece of Tm,Ho:YAG, is held in a copper clamp on the cold side of a TE cooler. The hot side is water-cooled with 10°C water, and running open-loop at a current of 5 A, a cold-side temperature of -30°C is routinely achieved. A thin Brewster plate ensures linear polarization, and two etalons working together force single-frequency operation. The laser consists of an aluminum box which encloses the laser crystal on its TE cooler. The box has two plexiglass sides to allow monitoring condensation buildup on the laser crystal. Attached to the box is an aluminum tube that contains the Brewster

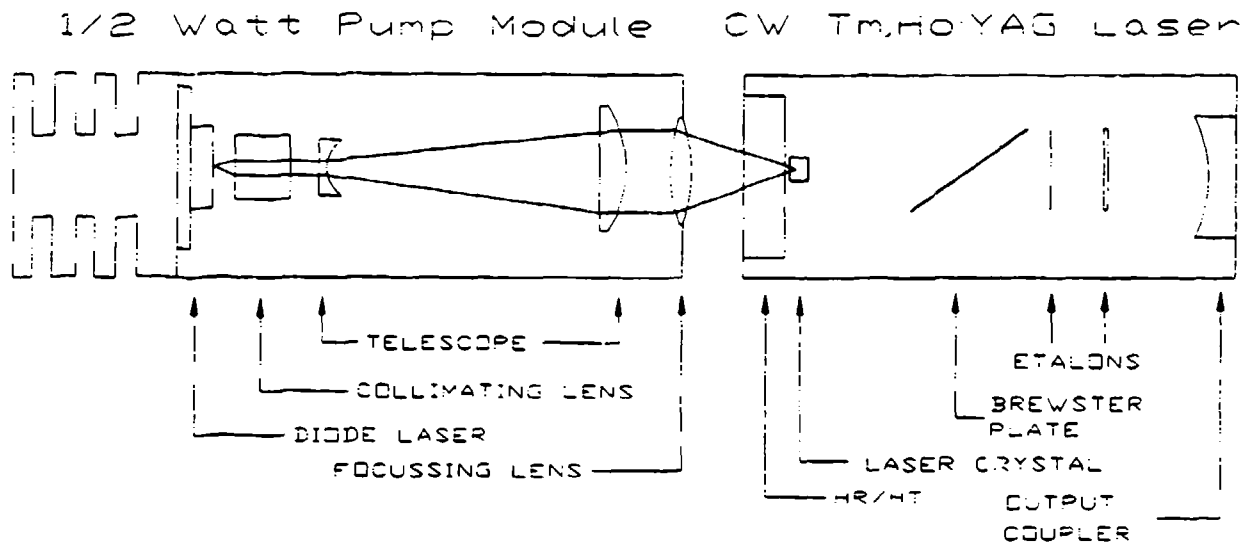


**Figure 9.** Schematic drawing of the CW Tm,Ho:YAG seed laser.

plate and the two etalons, mounted off-center on shafts that have hex-sockets to allow adjustment of the etalon angles. The output coupler is clamped to a spacer bolted to the end of the tube. The resonator is more rigid than one made with mirror mounts, and completely encloses the laser mode, preventing air currents from disrupting the laser frequency stability. The box is actively purged with dry nitrogen on initial cool-down, but once it has operated at  $-30^{\circ}\text{C}$  for a few minutes the gas flow can be turned off.

Figure 9 shows how the seed laser is pumped by a 500-mW diode laser module. The diode laser is mounted on an air-cooled heat sink, to which an 8.18-mm focal-length collimating lens is rigidly mounted. A double cylinder-lens telescope expands the collimated beam in the plane parallel to the diode junction, (shown in Figure 9) and contracts the beam in the nearly diffraction-limited plane (not shown). Then a 40-mm f.l. spherical lens focuses the beam into the Tm,Ho:YAG laser crystal. The focussing lens is adjustable over three degrees of freedom to optimize the overlap of the pumped volume with the hemispherical laser mode. This adjustment is the only one provided other than adjusting the angles of the etalons.

The performance of the seed laser as a function of diode pump-power is shown in Figure 10 for operation with no etalons, with the thin 0.17-mm etalon only, and with both the thin etalon and a 1-mm etalon. Adding the thin etalon only reduced the laser performance slightly, and the laser was tunable from  $2.089\ \mu\text{m}$  to  $2.098\ \mu\text{m}$  as measured with a small spectrometer with about 1 nm resolution. The  $2.121\ \mu\text{m}$  line was observed to run simultaneously with emission at  $2.093\ \mu\text{m}$ . Adding the 1-mm etalon to force single-frequency operation increased the laser threshold and reduced the maximum output considerably. It also severely

restricted the tunability of the laser, something we did not appreciate until later. The laser was still tunable over basically the same range, but only in discrete steps corresponding to the free-spectral-range of the 1-mm etalon. The frequency jitter was smaller than 1 MHz, the resolution of our interferometer, but the frequency drift was rather large, on the order of 1 MHz/s, due to the large thermal expansion coefficient of aluminum, and the fact that we had to use sub-ambient cooling water for the TE cooler, which slowly cooled the laser resonator. Future versions of this laser will have Invar resonators, and the hot side of the TE cooler will be insulated from the resonator.

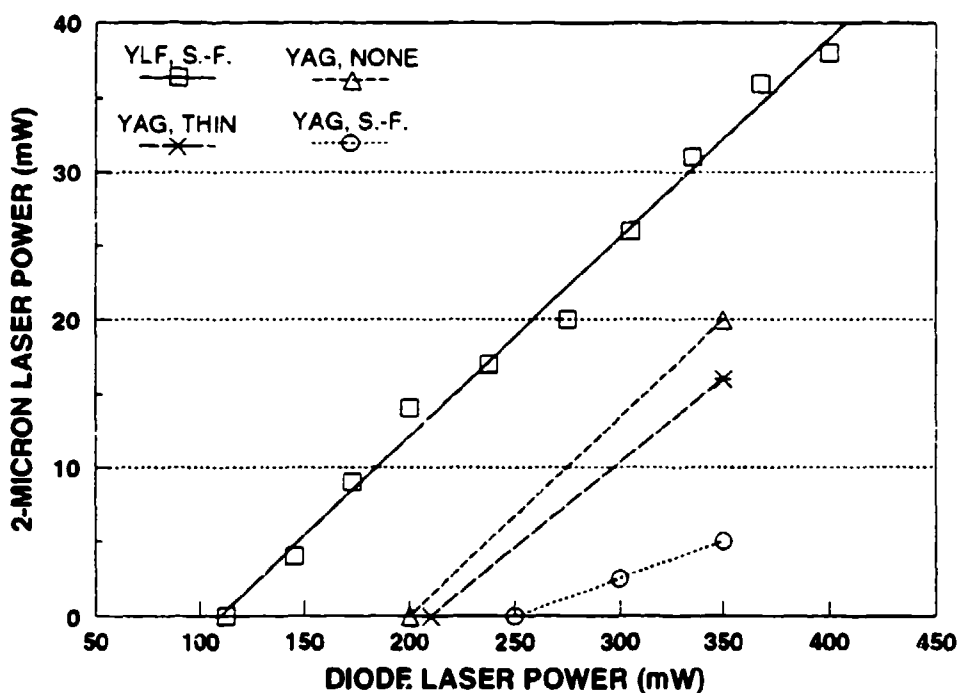


Figure 10. CW laser performance of the diode-pumped Tm,Ho:YAG laser operated with no etalons, with the thin etalon only, and single-frequency with both etalons. The single-frequency performance of our Tm,Ho:YLF laser is also shown.

### 3.2.2 Injection-Seeded Ring-Laser

We elected to begin the injection-seeding experiments using the ring-laser because the ring could be seeded through its output coupler, and because we would avoid the 30% energy penalty due to spatial hole burning. Disadvantages of using the ring included its higher misalignment sensitivity and concern over what would happen when the ring ran bidirectionally, sending a

Q-switched laser pulse directly into the isolator protecting the seed laser. We decided to go with the ring primarily because the seed-laser power was so low that we were not confident enough seed-power could be coupled into a standing-wave laser through an HR mirror.

Figure 11 is a scale drawing of the layout used for the seeding experiments. The major diagnostics are shown, as well as the amplifier which will be described in Section 3.3. Our original intention had been to move the seed-laser from its 1'x2' breadboard to the main 2'x4' breadboard, but as time was of the essence and we were not sure what the final configuration would be, we decided not to move it. The seed-laser output was collimated with a 100-mm f.l. lens, then reflected off a nominal HR@45° mirror to the main breadboard. The seed-laser power was monitored using the 1% transmission through the HR detected with a Judson InAs room-temperature detector. We had started the experiments with the Optics For Research isolator also mounted on the seed-laser breadboard, but we found that we had to move the polarizers some distance from the Faraday cell in order to achieve more than 10 dB of isolation. We measured over 30 dB of isolation with the arrangement shown in Figure 11. The seed-laser polarization was returned to horizontal with the 1/2 wave plate, then directed with two adjustable mirrors through the output coupler and into the laser rod, seeding the clock-wise direction. The seed was precisely aligned to the ring-laser mode using the infrared camera viewing through HR#3 and the InAs detector behind HR#1, the resonator mirror closest to the Q-switch. (The InGaAs detector was used to monitor the pulse-width and build-up time, and to look for mode-beating.) With the ring laser operating just below threshold, we would first steer the seed onto the same spot on the camera that the ring-laser hit, then maximize the fringe contrast on the InAs detector output displayed on an oscilloscope. Fringe contrast ratios greater than 10 were generated during the flashlamp pulse as the gain in the laser rod compensates for the cavity losses. We discovered that transient heating of the rod by each lamp pulse caused the cavity to sweep two to three modes each time the lamp was fired. Although not so surprising in retrospect, this realization forced us to abandon our plans to lock the ring to the seed using a CW feed-back loop developed and used successfully to seed a Ti:Al<sub>2</sub>O<sub>3</sub> laser. We also quickly found that air currents over the ring-laser caused the position of the fringes to jump wildly around, so we began to enclose and shield the resonator.

The initial experiments conducted with the above configuration proved to be unsuccessful. Although the ring would operate exclusively in the clock-wise direction, we saw no change in the degree of mode-beating and no change in the pulse build-up time as the voltage on the PZT was varied. We found the unidirectional behavior was due to retroreflection of the counter-clockwise beam off the seed-laser output coupler, in spite of the isolator. When we



verified with the small spectrometer that both lasers were operating on the 2.097  $\mu\text{m}$  line, there seemed to be a slight difference between the two lasers, not fully resolvable. We then transmitted a sample of the seed-output with a sample of the ring output through an optical fiber to a 0.64-m spectrometer in a separate room, and found that the two laser emissions were 0.27 nm apart. This is when we discovered that the seed-laser was no longer continuously tunable.

When we found that we could not tune the seed into coincidence with the ring, we inserted a thin film polarizer into the ring resonator, and attempted to tune the ring instead. We found that although we could not move the ring-wavelength into coincidence with the seed near 2.097  $\mu\text{m}$ , we could tune the ring near 2.091  $\mu\text{m}$  and into resonance with a different seed-laser output line. The ring was no longer operating on its lowest threshold transition, and the increase in threshold lamp energy forced us to reduce the repetition rate to 7 Hz and the pulse energy to 10 mJ. Injection-seeded operation could now be induced by adjusting the PZT voltage and monitoring the intensity of the reverse wave using the InAs detector shown just below the camera in Figure 11. We now found that the signal on this detector decreased by a factor of 16 when the ring ran in a single direction due to the retroreflection off the seed output coupler, and that it decreased another factor of 10 when seeding was successful. In addition, the width of the ring emission as detected by the 0.64-m spectrometer also decreased, and the mode pattern detected by the infrared camera went from smooth to highly modulated due to interference effects in the infrared vidicon tube window. The most compelling evidence for seeding was that the mode beating on the Q-switched pulse disappeared, and the pulse build-up time shortened by about 500 ns. Figure 12 shows two pulses captured by our Tektronix 7912AD digitizer using the same sweep delay, the early one a seeded pulse, the later one unseeded. Mode-beating is not apparent on either pulse because of the slow digitization rate required to span the range of buildup times. Figure 13 presents an unseeded and a seeded pulse captured at about 0.1 ns per digitized point, clearly showing the presence and absence of mode-beating. The sweep delay was individually adjusted to bring these pulses on screen. Based on how hard it was to maintain injection seeding by continuously adjusting the PZT voltage by hand, we estimate the seeding bandwidth to be on the order of 15-30 MHz. A pulse build-up time stabilization circuit under construction under a different program will be tested on this laser once it is completed.

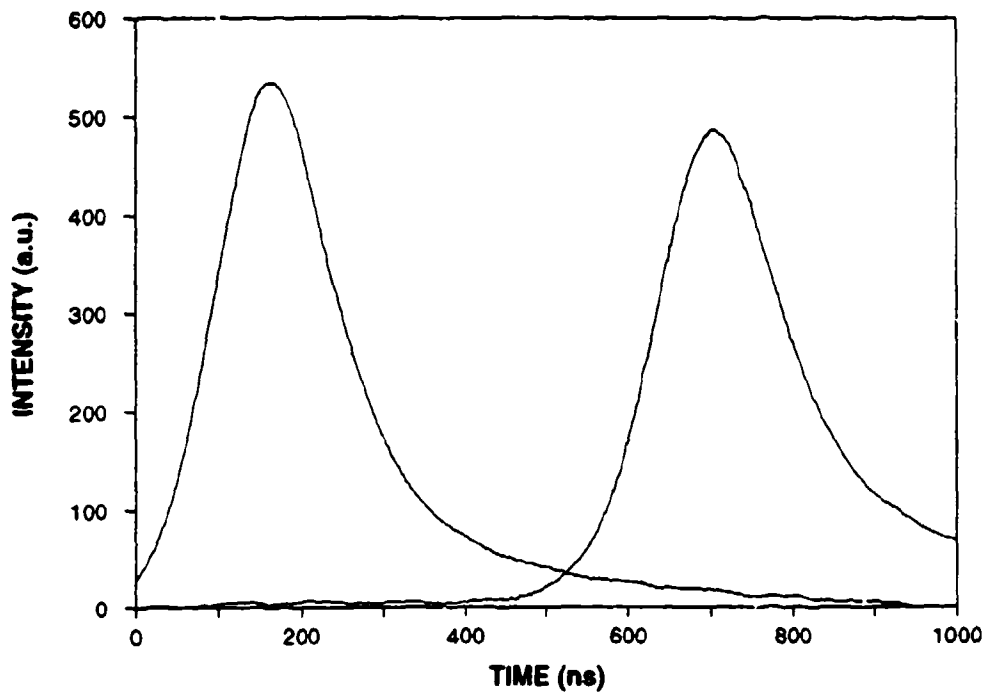


**Figure 12.** Seeded and unseeded laser pulses showing difference in build-up time.

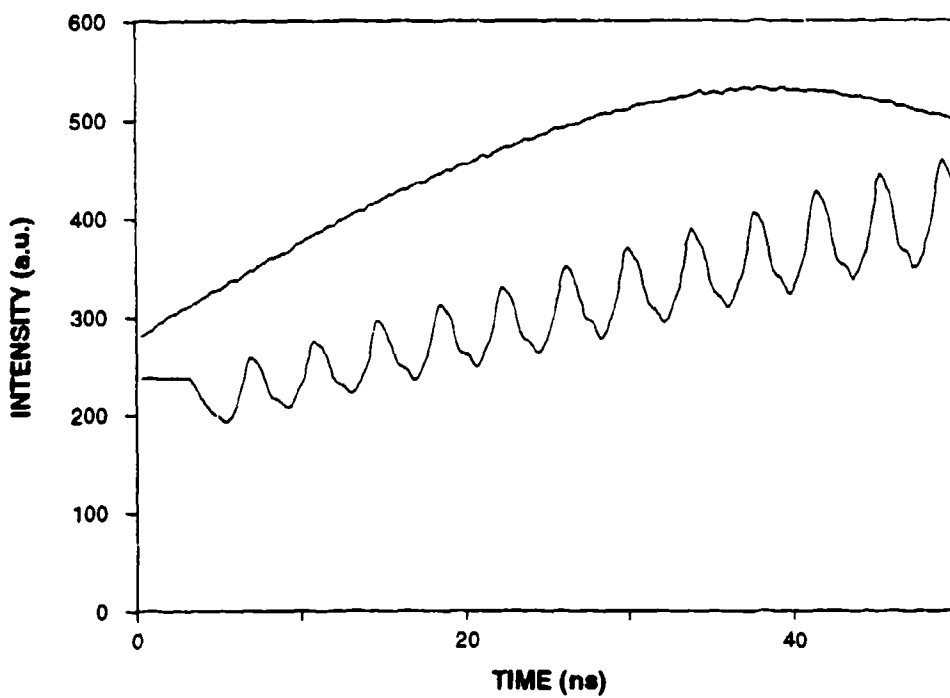


**Figure 13.** Seeded pulse with no mode-beating and unseeded pulse with mode-beating.

### 3.3 Task 3. Amplifier

3) *Develop a flashlamp-pumped amplifier capable of increasing the output of the above oscillator to 100 mJ/pulse, while preserving its TEM<sub>00</sub> SLM quality.*

Development of the amplifier proceeded in parallel with the first task as the pump-cavity and cooling system were optimized. We measured the small signal gain of the oscillator rod as a function of flashlamp energy and coolant temperature using an early version of the seed-laser. The large saturation fluence of holmium, over 10 J/cm<sup>2</sup>, means that for practical lamp-pumped amplifiers saturation will not be a concern, and the peak small signal gain we measured with the CW probe laser should be equal to the pulsed gain. To reach a net gain of five in a 10 cm rod, the gain coefficient,  $g_0$ , only needs to be 0.16 cm<sup>-1</sup>. As gain coefficients up to 0.18 cm<sup>-1</sup> had been reported in the literature, [2] we did not expect this task to be difficult.

We measured the single-pass small signal gain of rod H855 in pump cavity Version 2 using a CW 2.096- $\mu$ m laser. The strong thermal lens defocused the beam on the detector, making absolute gain measurement difficult, so instead we recorded the gain relative to the signal before the beginning of the lamp pulse. This quantity is the relative gain,  $G_{rel}$ . Figure 14 shows how the relative gain increased with pump energy at various coolant temperatures, all at 10 Hz. The true gain for the highest points on the graph was approximately three.

The small signal gain coefficient,  $g_0$ , can be calculated from  $G_{rel}$  using the absorption coefficient for ground state absorption. Accurate values as a function of temperature are not available, but reasonable relative values can be calculated from data collected in the earlier Phase II SBIR. Figure 15 presents  $g_0$  as a function of lamp energy calculated from the data in Figure 14. Note a slight curvature at high pump energies due to depletion of ground-state holmium ions, and the relatively small peak value of the gain coefficient.

Once injection seeding had been demonstrated as described in Section 3.2, we directed the ring-laser output through a second pump-cavity as shown in Figure 11. We used close-coupled cavity Version 3, cooled with Fluorinert, and collected data at 5°C and -30°C. Although we now had a 1 KV DC supply for our new lamp-driver, we were limited to using the same 0.5 ms current pulse-width as the oscillator because the new repetition-rate board was still under construction. Figure 16 presents the amplified pulse energy measured by the power meter represented by the solid square in Figure 11. The dashed line indicates the pulse energy measured in front of the amplifier. We pushed the lamp energy to nearly 140 J, and produced a net gain of three with the pump-cavity cooled to -30°C. We noticed that when the ring was seeded the output of the amplifier was significantly higher than when the ring was operating in

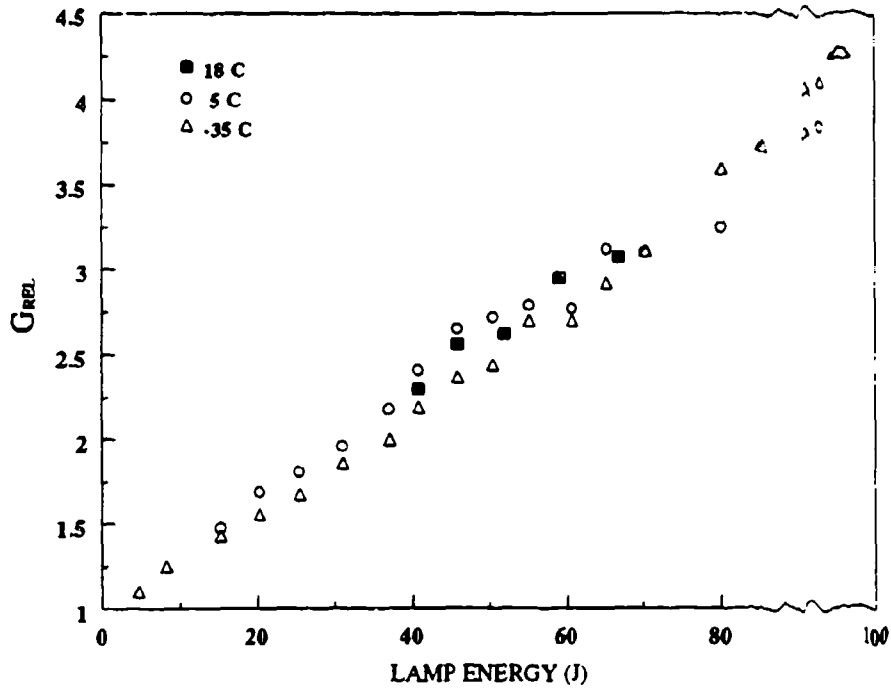


Figure 14. Relative gain measured at 2.096  $\mu\text{m}$  using a CW probe laser.

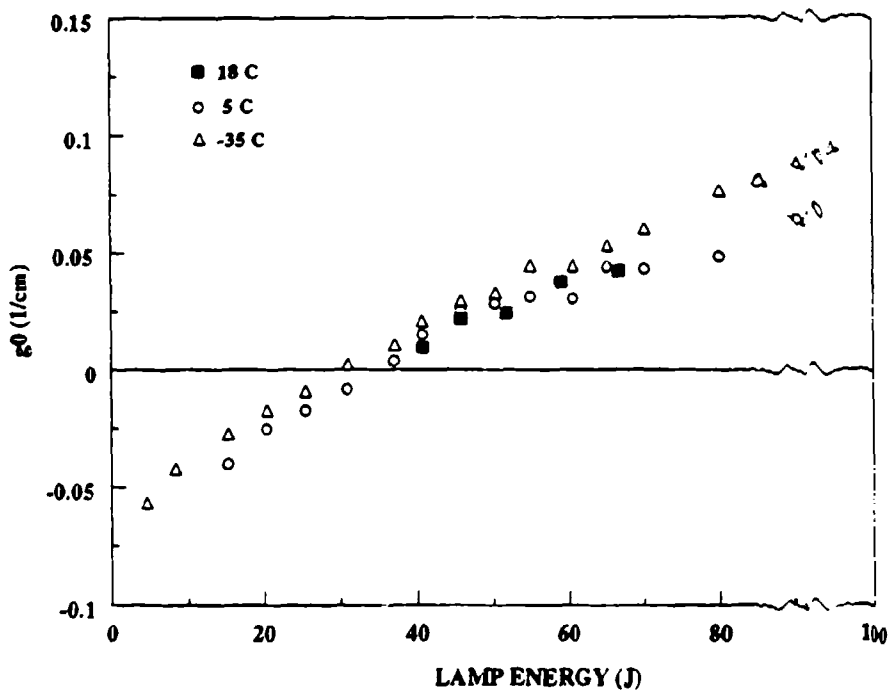


Figure 15. Small signal gain coefficient calculated from the data in Figure 14.

one direction but not single-frequency, even though the power meter placed in front of the amplifier could not detect this difference. The effect was most pronounced when the amplifier was cold, and may have something to do with operating the ring off line center, in order to be on resonance with the seed-laser.

Figures 17 and 18 present the amplifier gain and the small signal gain coefficient calculated from the data in Figure 16. Once again we were just barely able to achieve a gain of three, with a maximum calculated value for  $g_0$  of only  $0.12 \text{ cm}^{-1}$ . Although we expected the small signal gain to saturate at lamp energies around 100 J, we thought it would happen at  $g_0$  values closer to  $0.2 \text{ cm}^{-1}$ . We repeated these measurements using a  $250 \mu\text{s}$  lamp pulse and a variable delay relative to the Q-switched probe pulse, and got virtually identical results. This eliminates upconversion shortening of the Ho upper-state lifetime as the cause of the saturation, which leaves ground-state depletion as the likely culprit, again as expected. The low values of gain must then be due to a lower than expected Holmium concentration, or to being off line center. These measurements will have to be repeated with a probe laser firmly centered on the high-gain transition. Using a higher holmium concentration is also worth considering.

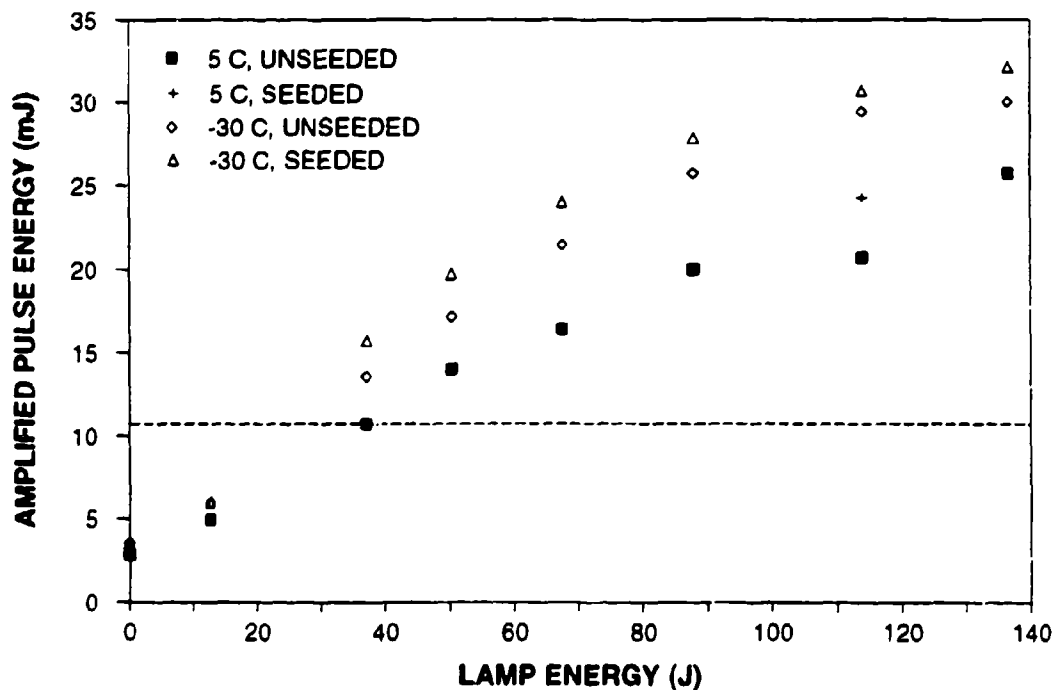


Figure 16. Amplified pulse energy measured at  $2.091 \mu\text{m}$  using the ring laser as the probe.

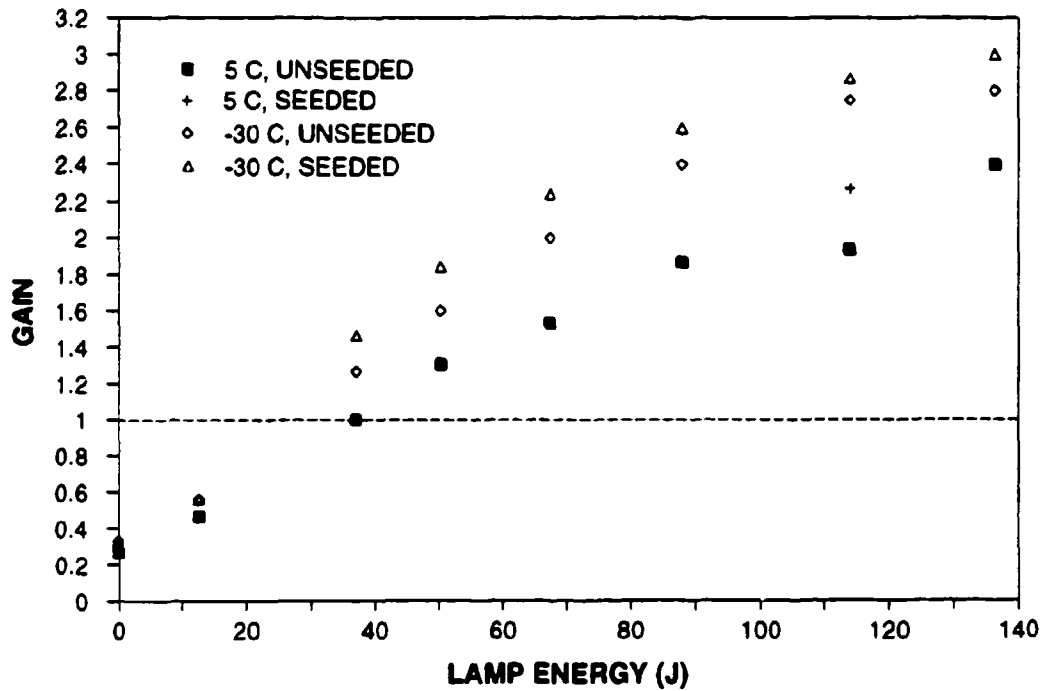


Figure 17. Absolute gain measured at 2.091  $\mu\text{m}$  using the ring laser as the probe.

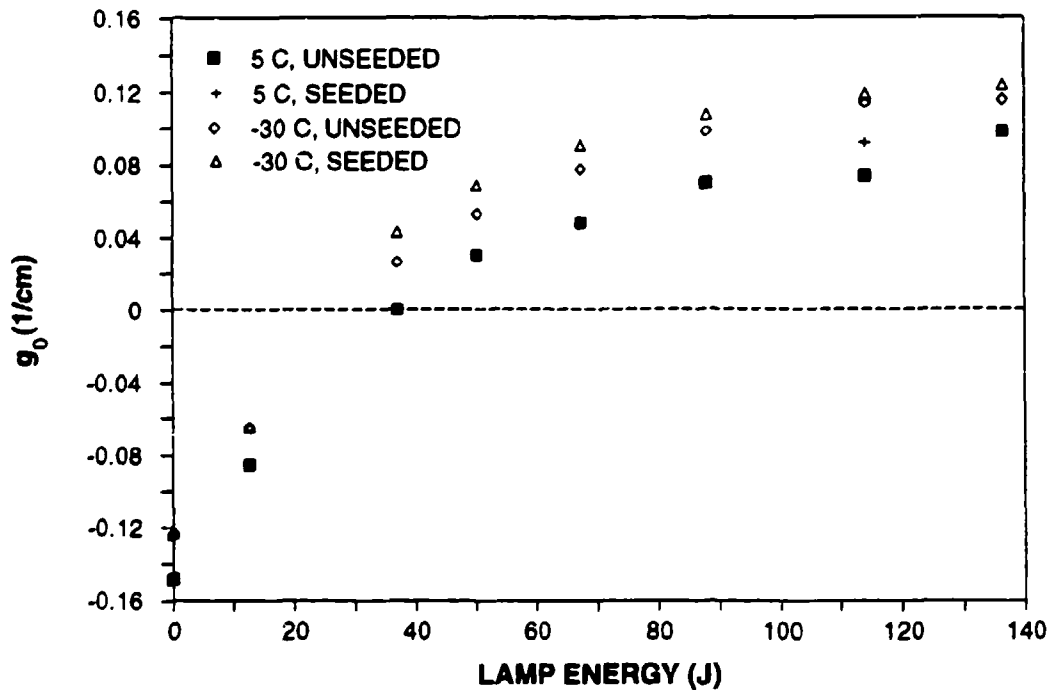


Figure 18. Small signal gain coefficient calculated from the gain data in Figure 17.

### 3.4 Task 4. Lidar Transmitter Design

- 4) *Design a ruggedized LIDAR transmitter incorporating a diode-pumped, SLM seed-laser, a Q-switched oscillator and an amplifier. Target specifications are 100 mJ at 10 Hz, SLM, TEM<sub>00</sub>, with a pulse-width between 500 ns and 1 μs.*

The design of the ruggedized transmitter was to begin once the first three tasks had been completed. The mechanical design was to be performed in consultation with persons familiar with the requirements of aircraft-qualified laser systems, and the design was to be presented to the Air Force for review in the form of a proposal for a follow-on contract. Unfortunately, we reached the end of the 18-month contract period with several outstanding issues remaining. However, if we summarize here our principal findings, we can show that a 100-mJ, 10-Hz transmitter is a realistic, if somewhat complex, possibility. We demonstrated a 30-mJ, 10-Hz oscillator in both a standing-wave and a ring configuration. Cooling the laser rod tends to shorten the laser pulse, but as long as 200 ns is acceptable, the reduced threshold leading to reduced thermal aberrations makes it worthwhile. The laser cavity has to be shielded from air currents for reliable seeding, so building a sealed, purged enclosure is not too much more difficult. We demonstrated injection-seeding of a ring resonator with no loss in output power from the unseeded case, so with a tunable seed-laser, 30 mJ @ 10 Hz should be achievable. This brings us to 90 mJ with the demonstrated gain of three in the amplifier. With a little more cooling, or perhaps operating on line center, 100 mJ is in reach.

### 4 References

1. S. W. Henderson, "Coherent Solid-State 1.06 and 2.1μm Lidar Systems for Wind Velocity Measurements", Paper EO4.2, OPTCON '90.
2. S. R. Bowman, M. J. Winings, S. Searles, and B. J. Feldman, "Basic Parameters for Cr,Tm,Ho:YAG 2.1μm Lasers", Paper SSL1.5/ThL5, OPTCON '90.